ISSN: 0973-3469, Vol.23, No.(1) 2026, Pg. 08-19

Material Science Research India

www.materialsciencejournal.org

Investigating the Electrochemical Performance of CuO-rGO for Methanol Oxidation in Alkaline Medium

CHANDRAMA SARKAR[1,2], SIMANTA DOLEY[3] and SWAPAN KUMAR DOLUI[1]*

[1]Department of Chemical Sciences, Tezpur University, Napaam, India
[2]Department of Chemistry, Pandit Deendayal Upadhyaya Adarsha Mahavidyalaya, Goalpara, India
[3]Department of Chemistry, Jengraimukh College, Majuli, India

Abstract

Using a hydrothermal process, we synthesized copper oxide supported on reduced graphene oxide (CuO-rGO) nanocomposites, which we then used as an electro-catalyst for the electro-oxidation of methanol. The CuO-rGO$_{calcined}$ nanocomposite shown good catalytic activity towards methanol electro-oxidation following calcination at 400 °C. Additionally, FTIR, XRD, Raman spectroscopy, SEM, EDX, and the dynamic light scattering (DLS) method were used to analyse the $_{calcined}$ composites. Cyclic voltammetry (CV) was used to assess the substances electrochemical analyses. The CuO-rGO$_{calcined}$ nanocomposite experiences irreversible methanol oxidation in an alkaline media. The nanocomposite has a lower positive characteristic peak (0.72 V) in the forward scan compared to CuO (0.75 V). Furthermore, the onset potential of the nanocomposites is lower than that of CuO, suggesting a reduction in the overpotential for methanol oxidation at the nanocomposites. The onset potential for the oxidation of methanol at the CuO-rGO$_{calcined}$ is around 0.44 V which is lower than that of several reported electrocatalysts such as CuO (ca. 0.46 V), Cu NW@rGO-GCE (ca. 0. 48 V), Cu NW-GCE (ca. 0. 6 V) poly-crystalline Cu-GCE (ca. 0.5 V), and Ni–Cu-GCE (ca. 0.5 V). Additionally, the peak current density at the CuO-rGO$_{calcined}$ nanocomposite is 2.4 times higher than that of CuO, suggesting the superior electro-catalytic activity of the nanocomposite. Chronoamperometry study reveals the exceptional durability and good tolerance against the oxidizing intermediate of the nanocomposites. The stability of the nanocomposite was further investigated for 100 continuous cycles. CuO-rGO$_{calcined}$ nanocomposite featuring high durability, low-cost and low onset potential reveals a superior catalytic activity for methanol electro-oxidation.

Article History
Received: 31 March 2026
Accepted: 15 June 2026

Keywords
Copper Oxide;
Electrocatalyst;
Methanol Electro-oxidation;
Nanocomposites;
Reduced Graphene Oxide;

CONTACT Swapan Kumar Dolui skdolui19@gmail.com Department of Chemical Sciences, Tezpur University, Napaam, India

Doi: http://dx.doi.org/10.13005/msri/230103

Abbreviations

DMFC	Direct methanol fuel cell
CuO	Copper oxide
GO	Graphene oxide
rGO	Reduced graphene oxide
FTIR	Fourier Transform Infrared Spectroscopy
XRD	X-ray diffraction
SEM	Scanning electron microscope
DLS	Dynamic light scattering
CV	Cyclic voltammetry

Introduction

The demand for a clean, affordable, and dependable energy supply is the basis of the world's growing economic success.[1] With the increase in energy demand along with the exhaustion of fossil fuels and the rapidly escalating environmental issues, the direct methanol fuel cell (DMFC) can be used as an alternate green and sustainable power source.[2] DMFC possesses several significant benefits compared to hydrogen-based fuel cells, such as great solubility in an aqueous electrolyte, good energy density, and raw materials that can be easily stored and distributed.[3] However, there are two major difficulties prohibiting DMFCs from effective commercialisation, which are expensive production and slow kinetics of the electro-oxidation of methanol at the anode.[4] Numerous studies have been conducted on various aspects of DMFC to address the problems that occurs in it.[5] Pt-based materials have been served widely as the effective single-metal catalyst for DMFCs.[6, 7] Unfavourably, its commercialization and practical application are severely hampered by its scarcity, high cost, low power density, and limited tolerance to CO poisoning.[8] Metal oxide-based catalysts were also used for DMFCs that effectively go via a bifunctional process and can provide hydroxyl sources at lower potentials.[9,10] Due to their low specific surface area, these catalysts suffer from poor electron conductivity. Their catalytic activity can be enhanced by incorporating them into different supporting materials. Carbon nanomaterials have attracted immense and persistent attention as electrode material for the various electrochemical performance because of their extraordinary chemical and physical properties.[11] Among various materials explored, graphene and its derivatives have emerged as highly active material for a wide variety of applications in various fields including fuel cells and other energy related applications.[12-14]

Metal oxide supported on graphene-based nanocomposites have gained great consideration due to their cheapness, durability, strong electrocatalytic activity, and simple production in DMFC applications. Graphene-based hybrid nanocomposites have been integrated into fuel cell applications with three major aspects *i.e.* electrocatalysts, electrolytes, and gas diffusion layers.[19-21] Copper oxide (CuO), a well-known p-type semiconductor material, has potential in various applications such as gas sensors[22], CO oxidation catalysts[23], solar energy conversion[24], lithium-ion battery anode materials[25], magnetic phase transmitters[26], heterogeneous catalysts[27], optical switches[28], nanofluids[29] and field emitters[30] because of their high catalytic activity as well as their nontoxic nature and affordable cost.[31] Incorporation of CuO nanoparticles onto graphene surface can improve the electrochemical performance of the nanocomposite in comparison with the pure nanoparticles. Mai et. al[32] have synthesised a CuO-graphene composite from CuO and graphene oxide (GO) and used it as anode material for lithium-ion batteries. The synergetic effect of CuO and GO is beneficial for the improved electrochemical performances of CuO-graphene based composites. Abdul Waheed et. al[33] has synthesised structure-controlled Cu_2O graphene nanocomposites and studied their photocatalytic activity. As far as our knowledge, there is no reported work in the literature regarding the electrocatalytic application of CuO-rGO towards DMFC. However, researchers have reported several Pt/metal oxide/graphene composites for DMFCs, including Pt/CeO/graphene, Pt/MnO_2/graphene, and Pt/TiO_2/graphene, in which metal oxide serves as a co-catalyst.[34, 35] Therefore,

the main objective of this work is to synthesise a low-cost Pt free electrocatalyst for effective oxidation of methanol.

In this work, CuO-rGO is calcined at 400 °C and used as an electrocatalyst for DMFCs. Interestingly, in an alkaline media, the calcined nanocomposites demonstrated strong electrocatalytic activity for methanol electro-oxidation.

Materials and Methods

Chemicals

Graphite powder, (<20 micron) was purchased from Aldrich. $KMnO_4$, $NaNO_3$, H_2O_2, (30%), CuCl, sodium hydroxide (NaOH), conc. H_2SO_4, HCl and methanol were procured from Merck. Nafion solution was purchased from Sigma-Aldrich.

Synthesis of GO

The Modified Hummers method was used to synthesize GO from natural graphite.[36] While maintaining vigorous stirring, part by part mixing of the chemicals; Graphite powder (5 g), $NaNO_3$ (5 g) and 120 mL of H_2SO_4 (98%) were carried out in a 500 mL flask. After 30 minutes of stirring in an ice bath, 30 g of $KMnO_4$ was added to the mixture. After removing the ice bath, the mixture was left to stir at room temperature for the entire night. The liquid progressively took on the consistency of paste as the reaction went on, and its colour changed to a light brownish. Finally, the mixture was heated to 98°C while being vigorously stirred, and 300 mL of water was gradually added. The diluted suspension was stirred overnight giving a yellow sample. Then, 100 mL of 30% H_2O_2 was added to the mixture under continuous stirring at room temperature. The mixture was purified by rinsing it, centrifuging it with 5% HCl, and then repeatedly using deionized (DI) water. A grey-colored GO powder was produced following filtration and vacuum drying.

Synthesis of CuO-rGO Nanocomposite

The CuO–rGO nanocomposite was prepared using a hydrothermal approach with minor modifications from previously reported methods.[37] Initially, 10.0 mg of GO was dispersed in 10.0 mL of distilled water, while 9.89 mg of CuCl (corresponding to 0.01 mol CuCl per 1000 mg of GO) was separately dissolved in 20 mL of distilled water. Both solutions were subjected to ultrasonication to obtain a uniform and stable dispersion. The CuCl solution was then gradually supplemented with the GO dispersion. After 120 minutes of magnetic stirring at 25 °C, the solution combination was put into a 50 mL autoclave. After the mixed solution was hydrothermally treated for four hours at 150 °C, the solid result was repeatedly centrifuged and cleaned with distilled water. The requisite CuO-rGO nanocomposites were then obtained by drying the composites at 100 °C.

Synthesis of CuO-rGO$_{calcined}$ Nanocomposite

The synthesized CuO-rGO nanocomposite by using above mentioned procedure was calcined at 400°C for 30 min (labelled as CuO-rGO$_{calcined}$) and used for electrochemical applications. The calcination of the nanocomposite at 400 °C for 30 minutes is carefully chosen to achieve a balance between forming a pure phase, optimal crystallinity, effectively reducing the GO into rGO for the specific application of the CuO-rGO nanocomposite in the field of catalysis.

For comparison, CuO nanoparticles were synthesized via the direct thermal decomposition method with little modification.[38]

Characterization

The synthesized materials were analyzed using FTIR, XRD, SEM, and EDX techniques. FTIR measurements were performed on a Nicolet Impact 410 spectrophotometer within the wavenumber range of 4000–500 cm^{-1} using KBr pellets. XRD studies were conducted at ambient temperature (~298 K) with a Rigaku diffractometer employing Cu-Kα radiation (λ = 0.15418 nm), operated at 30 kV and 15 mA. The diffraction data were collected over a 2θ range from 10° to 70° at a scanning rate of 0.05° s^{-1}. The morphology of GO, CuO, CuO-rGO and CuO-rGO$_{calcined}$ nanocomposite were characterized with scanning electron microscope (SEM). The JSM-6390LV (Jeol, Japan) Scanning Electron Micrograph equipped with an energy dispersive X-ray detector was used for the SEM characterizations at an accelerating voltage of 15–20 kV and magnifications of ×15,000 and ×20,000. The particle size distribution was studied using Micritrac Flex Software by Dynamic light scattering (DLS) method. The electrochemical analyses were carried out by cyclic voltammetry (CV) using Bio Logic Science Instrument, SP-150 and Power: 110-240 Vac voltammeter.

Electrochemical Measurements

The electrochemical analyses of the prepared samples were studied using a standard one compartment three electrodes cell where Pt and Ag/AgCl electrodes were used as counter and reference electrodes respectively. The working electrode was a glassy carbon electrode (6 mm diameter) above which the catalyst paste was applied which was prepared by dispersing 12.5 mg of electrocatalyst in 0.5ml of ethanol by ultrasonication for 30 min. Then 0.025mL of 5 wt% Nafion was added onto the paste and air dried for 24h. To measure the methanol electro-oxidation, CV was performed between -0.2 V to 0.9 V at a scan rate of 50 mVs^{-1} in 0.1 M NaOH containing 1 M methanol. To measure the stability of the electrocatalyst the chronoamperometry study was performed for 600 s at a fixed potential of 0.4 V. The durability of the catalyst was further investigated for 100 continuous cycles at scan rate of 50 mVs^{-1}.

Results

FTIR Study

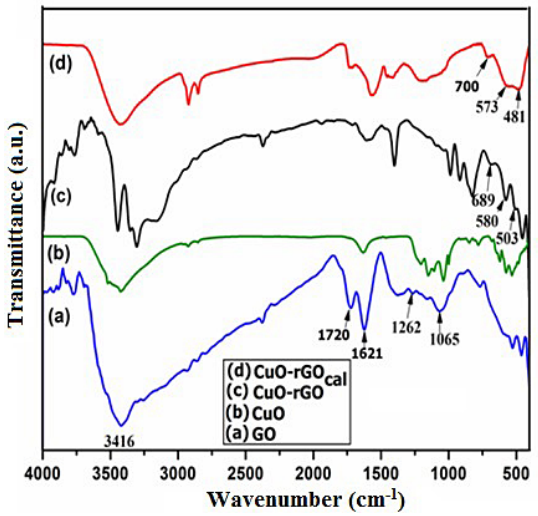

Fig.1: FTIR spectrum of (a) GO, (b) CuO, (c) CuO-rGO and (d) CuO-rGO$_{calcined}$ nanocomposite

XRD Analysis

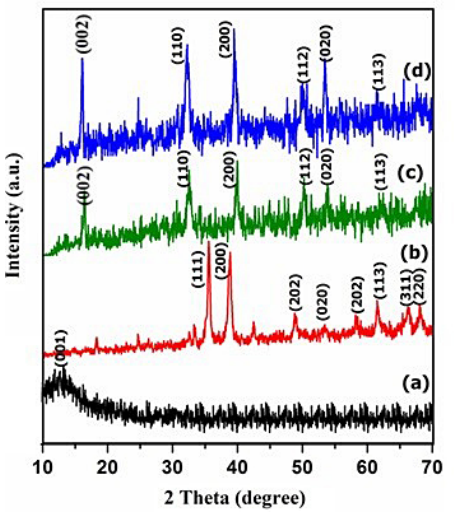

Fig. 2: XRD spectrum of (a) GO, (b) CuO, (c) CuO-rGO and (d) CuO-rGO$_{calcined}$ nanocomposites

Raman Analysis

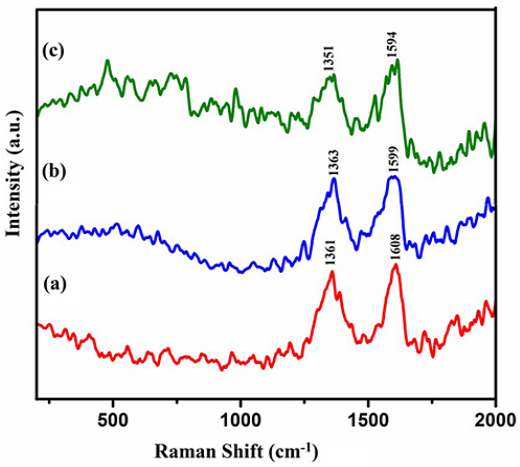

Fig. 3: Raman spectra of (a) GO, (b) CuO-rGO and (c) CuO-rGO$_{calcined}$ nanocomposites

Discussion

FTIR Study

Fig. 1 presents the FTIR spectra of GO, CuO, CuO–rGO, and calcined CuO–rGO nanocomposites. In GO, the peaks at 1720 cm^{-1}, 1262 cm^{-1}, and 1065 cm^{-1} correspond to C=O, epoxy C–O, and alkoxy C–O stretching vibrations, respectively (Fig. 1a). The bands at 1621 cm^{-1} and 3416 cm^{-1} are assigned to aromatic C=C and O–H stretching vibrations. For CuO nanoparticles, characteristic absorption bands appear in the 500–700 cm^{-1} region due to Cu–O vibrations (Fig. 1b). In the CuO–rGO composite,

the intensity of oxygen-related functional groups decreases significantly, indicating reduction of GO. At the same time, new peaks appear around 689 cm^{-1}, 580 cm^{-1}, and 505 cm^{-1}, confirming the presence of Cu–O bonds and successful formation of the composite (Fig. 1c). After calcination, these Cu–O peaks shift slightly to 700 cm^{-1}, 573 cm^{-1}, and 481 cm^{-1}, suggesting structural changes and stronger interaction between CuO and rGO (Fig.1d). The bands above 1500 cm^{-1} in the FTIR spectra of composite mainly arise from oxygen functional groups, carbon backbone and adsorbed hydroxyl groups present on rGO sheets.

SEM and EDX Analysis

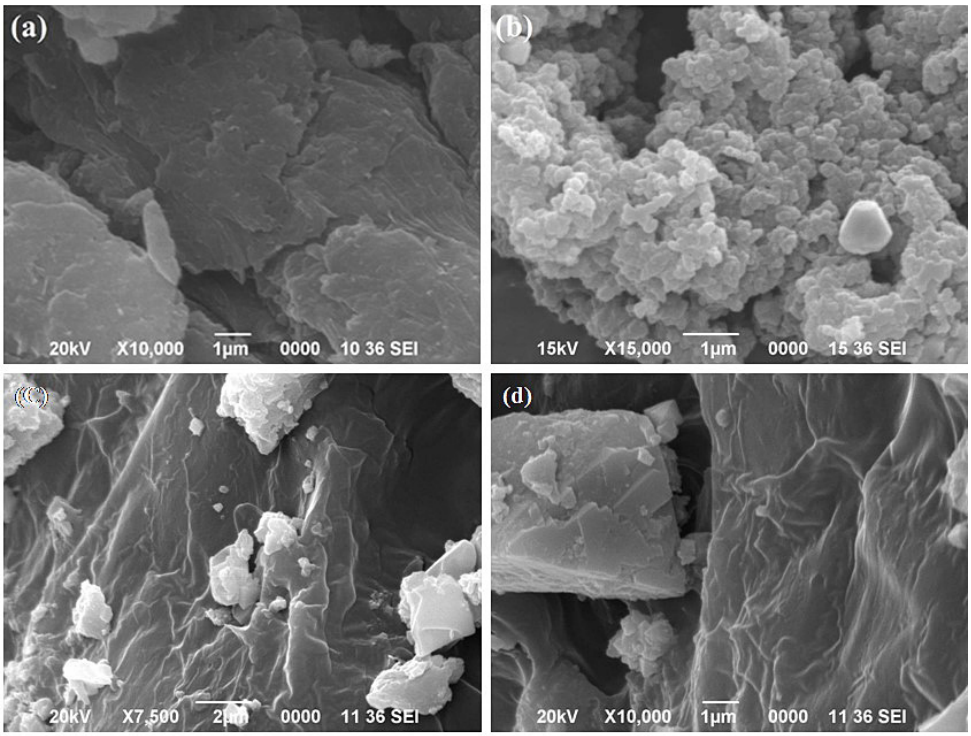

Fig. 4: SEM images of (a) GO, (b) CuO, (c) CuO-rGO and (d) CuO-rGO$_{calcined}$ nanocomposite

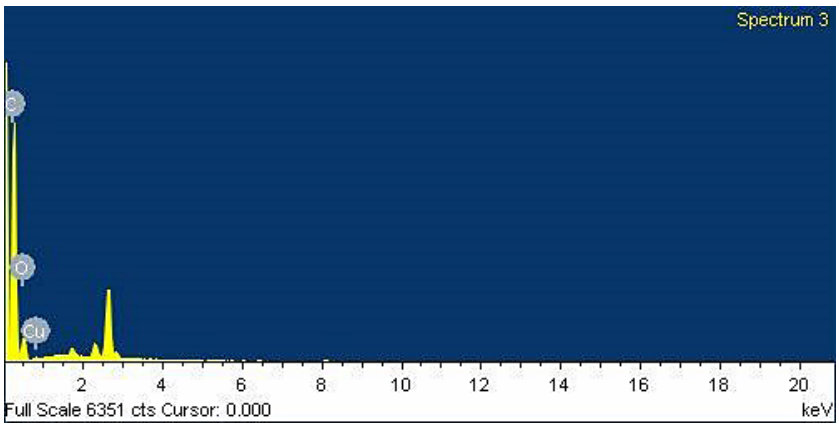

Fig. 5: EDX spectrum of CuO-rGO$_{calcined}$ nanocomposites

Particle Size Distribution

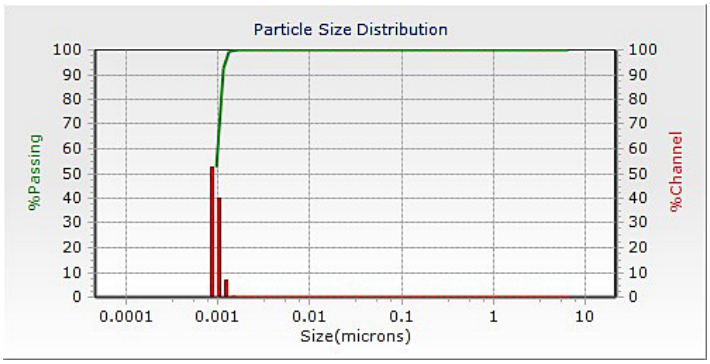

Fig. 6: Particle size distribution of CuO-rGO$_{calcined}$ nanocomposite

Electrocatalytic Oxidation of Methanol

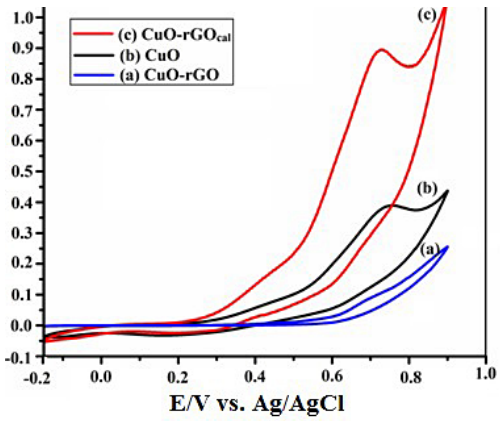

Fig. 7: CVs of the (a) CuO-rGO, (b) CuO and (c) CuO-rGO$_{calcined}$ in 1.0 M methanol solution containing 0.1 M NaOH. Scan rate: 50 mV s-1.

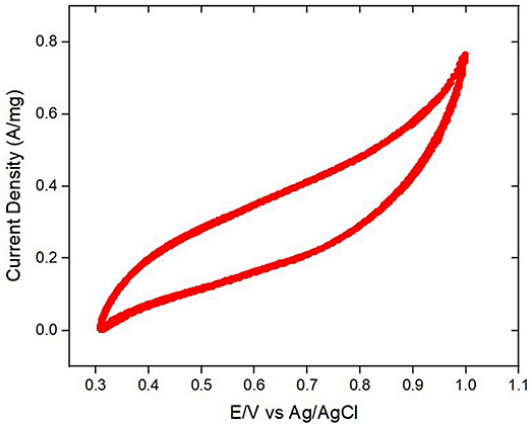

Fig. 8: CVs of the rGO in 1.0 M methanol solution containing 0.1 M NaOH. Scan rate: 50 mV s-1.

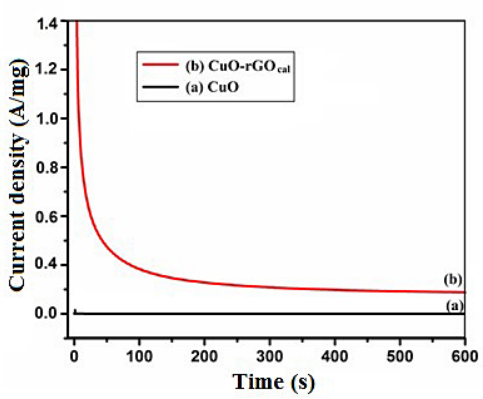

Fig.9 Chronoamperograms of (a) CuO and (b) CuO-rGO$_{calcined}$ for methanol oxidation in methanol solution (1.0 M) containing 0.1 M NaOH

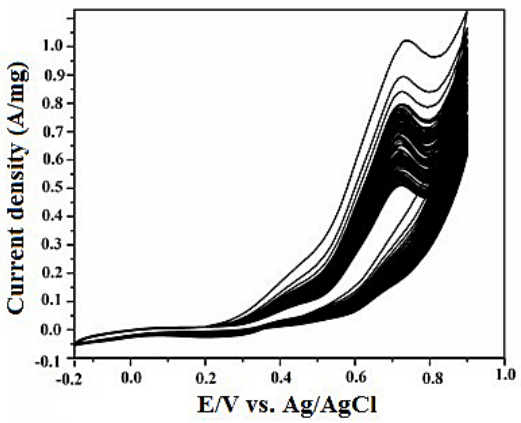

Fig. 10: CVs of the CuO-rGO$_{calcined}$ in 1.0 M methanol solution containing 0.1 M NaOH at scan rate: 50 mV s-1 for 100 cycles.

The shifting of intensity peaks for the Cu-O stretching vibrations after calcination of CuO-rGO nanocomposite is due to changes in the crystallinity, particle size, and the removal of oxygen-containing functional groups and organic residuals. Calcination helps to remove defects and reduces micro-strain, which causes a shift in the Cu-O absorption peaks. Calcination also influences the interaction between the CuO nanoparticles and the rGO sheets. Shifts in the Cu-O peaks reflect the strengthening of the interfacial interaction between the CuO and the crGO matrix as they settle into a more stable composite structure.

XRD Analysis

XRD analysis acts as the structural blueprint that directly predicts how well the material will perform during electrochemical reactions. High crystallinity is important for electro-oxidation because it improves charge transport and electron mobility during methanol oxidation. Fig. 2 shows the XRD pattern of GO, CuO, CuO-rGO and CuO-rGO$_{calcined}$ nanocomposite. A significant diffraction peak in GO was seen at 2θ= 11.53° (Fig. 2a), which was assigned to the (001) plane by functional groups containing oxygen on carbon sheets. The positions of the diffraction peaks in the XRD patterns of CuO, CuO, CuO-rGO, and CuO-rGO$_{calcined}$ agreed well with standard CuO and rGO. In the XRD spectrum of CuO, the major peaks located at 2θ=35.62° and 38.9° indexed as (111) and (200) planes, respectively, are corresponding to the pure monoclinic end-centered CuO crystal lattice (Fig. 2b). Peaks in the XRD spectrum of CuO-rGO at 2θ values of 18.3° (002), 32.49° (110), 39.76° (200), 50.32° (112), 53.6° (020), and 61.59° (113) are consistent with the typical XRD measurements for the end-centered crystal lattice's CuO monoclinic phase (Fig. 2c). Additionally, the spectrum shows small peaks at 25.2° and 44.85° which could be assigned to rGO (Fig. 2c). After calcinations, in the XRD spectrum of CuO-rGO$_{calcined}$ the peak intensities of the observed peaks increased hence crystallinity of the composite increases without any peak shifting (Fig. 2d). Therefore, CuO-rGO$_{calcined}$ becomes notably crystalline after calcinations. The appearance of lattice distortions in both your uncalcined and calcined CuO-rGO samples is indicator of successful chemical integration. In the uncalcined CuO-rGO, distortions manifest primarily as peak broadening, peak shifts, or baseline distortions due to the messy, room-temperature nucleation process. While in the calcine sample, thermal energy is used to grow crystals, yet distortions remain or even evolve because of thermal and chemical interactions.

Raman Analysis

Raman spectroscopy is often employed to characterize graphitic materials since it a useful technique for studying disorder ess and defects in crystal structure. The ratio of intensities of the D and G bands (ID/IG) obtained from Raman spectra is commonly used to evaluate the level of structural disorder in graphitic materials. Fig. 3 presents the Raman spectra of GO, CuO–rGO, and calcined CuO–rGO samples. The G bands appear at 1608 cm^{-1}, 1599 cm^{-1}, and 1594 cm^{-1}, while the D bands are observed at 1361 cm^{-1}, 1363 cm^{-1}, and 1351 cm^{-1} for GO, CuO–rGO, and CuO–rGO$_{calcined}$ samples, respectively. The G band originates from the in-plane vibration of sp²-hybridized carbon atoms in a hexagonal lattice, corresponding to the $E_{2}g$ mode of graphite. In contrast, the D band is associated with structural defects and edge sites, indicating disruption of the sp² carbon network and partial conversion to sp³ hybridization. The calculated ID/IG ratio for GO is 0.82, reflecting a significant degree of disorder introduced during the oxidation of graphite. For the CuO–rGO and CuO–rGO$_{calcined}$ samples, the ratios increase to 1.01 and 1.0, respectively, suggesting the introduction of additional defects and structural distortions upon incorporation of CuO. Meanwhile, the change in the nanocomposite's intensity ratio relative to the GO indicates a partial reduction of the GO. Furthermore, to the G and D band, there are three additional weak peaks at 282, 338, and 599 cm^{-1} in the Raman spectrum of CuO-rGO and CuO-rGO$_{calcined}$ which belong to A_g and $2B_g$ CuO phonon peaks.[39] After calcination, the Ag and 2Bg peaks migrated slightly to higher wave numbers and sharpened. These results also established the presence of both rGO and CuO in the prepared nanocomposites.

Since the D and G bands are characteristic features of graphitic carbon materials and therefore remain visible after CuO incorporation. However, changes in the ID/IG ratio and the appearance of CuO peaks confirm successful formation of the CuO–rGO composite and structural modification after calcination.

SEM and EDX Analysis

The morphological changes that occurred on the surface of GO due to incorporation of CuO nanoparticle was examined by SEM analysis. Fig. 4 shows the SEM images of GO, CuO, CuO-rGO and CuO-rGO$_{calcined}$ nanocomposite. The surface of GO shows a leaf like crumpled structure (Fig. 4a) while CuO shows spherical structure (Fig. 4b). It is seen that CuO and CuO-rGO nanocomposite surfaces exhibit different surface morphologies. CuO nanoparticles are evenly dispersed across GO's crumpled, paper-like surface, confirming their integration into GO. (Fig. 4c). From this it can be concluded that calcination enhances surface morphology. Highly uniform nano-spherical CuO could be observed for the CuO-rGO$_{calcined}$ nanocomposite (Fig. 4d).

The leaf-like and crumpled surface morphologies observe in the SEM images of the composites rather than clean, uniform spheres are strong confirmation of a highly successful CuO-rGO composite formation. For electrocatalytic applications, these irregular shapes are significantly more beneficial than perfect spheres because it increases the effective surface area, prevents nanoparticle agglomeration, and exposes more active catalytic sites for methanol oxidation.

EDX is the only technique that explicitly tells what elements are present and exactly how they are distributed. For a CuO-rGO electrocatalyst, EDX is indispensable for verifying elements and detecting contaminants. It proves the successful presence of Cu and O from the oxide, alongside carbon (C) from the rGO support (Fig. 5).

Particle Size Distribution

The particle size distribution of CuO-rGO$_{calcined}$ nanocomposite is shown in Fig. 6. The diameter of the nanocomposite ranged from 0.00096 to 0.00122 micron and the mean diameter is 0.001 micron. The size of CuO-rGO$_{calcined}$ nanocomposite is extremely small but scientifically plausible, provided specific synthesis methods are used and the measurement technique is reliable. This dimension approaches the quantum dot regime and presents both unique properties and measurement challenges. The rGO sheets can act as a scaffold, providing numerous nucleation sites and physically confining the growth of the CuO nanoparticles, thereby preventing agglomeration and promoting the formation of ultrafine nanoparticles.

Electrocatalytic Oxidation of Methanol

CV is a core component of electrochemical instruments for the majority of experimental studies in basic electrochemistry analysis. It produces two key outcomes of electrochemical reactions: the onset potential and the oxidation potential. The onset potential, which shows the potential at which a redox reaction starts, and the oxidation potential, which shows the peak current connected to the potential that oxidizes the analyte. These metrics offer important information for assessing an electrocatalyst's catalytic energetic performance. The oxidation potential, which indicates the energy needed for the analyte's oxidation process, represents the overall efficiency of the reaction, but the onset potential, in particular, is a crucial measure of the catalyst's efficacy in starting the intended reaction. The onset and oxidation potentials are very crucial to understand the reaction kinetics, electron transfer rates, and energy requirements across various electrochemical reactions.

The electrocatalytic performance of CuO, CuO-rGO and CuO-rGO$_{calcined}$ was studied via CV in alkaline media**.** Fig. 7 illustrates the CV of the CuO, CuO-rGO and CuO-rGO$_{calcined}$ measured in 1.0 M methanol solution containing 0.1 M NaOH. CuO-rGO$_{calcined}$ and CuO show distinct anodic peak towards forward scan, however, there is no characteristic peak for CuO-rGO. This indicates that after calcinations, CuO-rGO nanocomposites show catalytic activity towards methanol electro-oxidation. For comparison, CV analysis of rGO was recorded under the same experimental conditions (Fig.8). Due to its electrochemical double layer capacitor (EDLC) nature, the rGO exhibit a roughly rectangular CV curve; nevertheless, they lack an anodic peak. The superior electrocatalytic activity was provided by the CuO-rGO$_{calcined}$ nanocomposite for the electro-oxidation of methanol in alkaline medium. During the forward scan, CuO-rG O$_{calcined}$ shows a distinguishing peak at ca. 0.72 V for the oxidation of methanol, which is lower than that of CuO (0.75 V). A single oxidation peak is generated, revealing the irreversible methanol oxidation. The onset potential for the oxidation of methanol at the CuO-rGO$_{calcined}$ is around 0.44 V in an alkaline medium, which is lower than that of the CuO (ca. 0.46 V), Cu NW@rGO-GCE

(ca. 0. 48 V), Cu NW-GCE (ca. 0. 6 V) poly-crystalline Cu-GCE (ca. 0.5 V), and Ni–Cu-GCE (ca. 0.5 V).[40] Additionally, the peak current density for methanol oxidation at the CuO-rGO$_{calcined}$ (0.89 mA μg^{-1}) is 2.4 times greater than that of CuO (0.37 mA μg^{-1}), indicating the composite's better electrocatalytic activity. The onset potential and peak potential at the CuO-rGO$_{calcined}$ changed toward a less positive potential in comparison to the CuO nanoparticle, suggesting a decrease in the overpotential for methanol oxidation. Basically, methanol oxidation occurs more rapidly at CuO-rGO$_{calcined}$ surface. The synergistic effects of CuO and the conductive rGO support—improved conductivity and surface area of rGO sheets that facilitate greater CuO nanoparticle anchoring are responsible for the increased catalytic activity.[41] Moreover, the uniform distribution rough and the surface morphology of nano CuO improved the catalytically active sites.

Methanol underwent electro-oxidation in alkaline solutions via a facilitated electron transfer mechanism. Cu^{III} species produced during the anodic sweep finish the oxidation process by reacting with intermediates such CO and OH-like species.

$$Cu^{II} \leftrightarrow Cu^{III} + e^-$$
$$Cu^{III} + (CH_3OH)_{ads} \rightarrow \text{intermediate} + Cu^{II}$$
$$Cu^{III} + \text{intermediate} \rightarrow \text{product} + Cu^{II}$$

The durability of CuO-rGO$_{calcined}$ and CuO was evaluated by chronoamperometry (Fig.9) for 600s. At the CuO-rGO$_{calcined}$, a little decline in the current density was seen within the first 200s, which is related to the intermediates of methanol oxidation that adsorb on the catalyst surfaces.[42] The current density then stabilised for the duration of the testing time after reaching a steady state. It was observed that the CuO-rGO$_{calcined}$ electrode had a greater current density than the CuO electrode, demonstrating the composite's exceptional toughness, strong tolerance to oxidised intermediates, and good catalytic activity for the electro-oxidation of methanol. The stability of the CuO-rGO$_{calcined}$ electrode was further investigated for 100 continuous cycles. The voltammetric response decreased slowly with the increasing cycles (Fig. 10).

Conclusion

Under alkaline conditions, the synthesized nanocomposite demonstrated more electro-catalytic activity towards methanol electro-oxidation than CuO nanoparticles. At the CuO-rGO$_{calcined}$ surface, the nanocomposite experiences irreversible methanol. The nanocomposites' starting potential is lower than CuO, indicating a decrease in the overpotential for methanol oxidation at the nanocomposites. Furthermore, the peak current density at the CuO-rGO$_{calcined}$ nanocomposite is 2.4 times greater than that of CuO, indicating the nanocomposite's better electro-catalytic activity. The remarkable endurance and high tolerance of the nanocomposites against the oxidizing intermediate are revealed by the chronoamperometry investigation. Superior catalytic activity for methanol electro-oxidation is revealed by a CuO-rGO$_{calcined}$ nanocomposite with good durability, cheap cost, and low onset potential.

Acknowledgement

The authors gratefully acknowledge Tezpur University for providing the necessary support and facilities to carry out this research work. The authors also extend their thanks to all individuals who directly or indirectly contributed to this study.

Funding Sources

The author(s) received no financial support for the research, authorship, and/or publication of this article.

Conflict of Interest

The authors do not have any conflict of interest.

Data Availability Statement

This statement does not apply to this article.

Ethics Statement

This research did not involve human participants, animal subjects, or any material that requires ethical approval.

Informed Consent Statement

This study did not involve human participants, and therefore, informed consent was not required.

Clinical Trial Registration

This study did not require any clinical trials. So, this is not applicable to this research paper.

Permission to reproduce material from other sources

Not Applicable.

Author Contributions

- **Chandrama Sarkar:** Conceptualization, Methodology, Writing – Original Draft.
- **Simanta Doley:** Data Collection, Analysis, Writing – Review & Editing.
- **Swapan Kumar Dolui:** Funding Acquisition, Resources, Supervision.

References

1. Chu S, Majumdar A. Opportunities and challenges for a sustainable energy future. *Nature.* 2012;488:294. doi:10.1038/nature11475
2. Osman SH, Kamarudin SK, Shaari N *et al*. Review on Direct Methanol Fuel Cells: Bridging the Gap between Theory and Application for Sustainable Energy Solutions, *Energy & Fuels* 2025;*39*:12. doi:10.1021/acs.energyfuels.4c05357
3. Rodriguez-Reinoso F. The role of carbon materials in heterogeneous catalysis. *Carbon.* 1998;36:159. doi:10.1016/S0008-6223(97)00173-5
4. Chen CY, Chang JK, Tsai WT, Hung CH. Uniform dispersion of Pd nanoparticles on carbon nanostructures using a supercritical fluid deposition technique and their catalytic performance towards hydrogen spillover. *J Mater Chem.* 2011;21:19063. doi:10.1039/C1JM13461A

5. Alias MS, Kamarudin SK, Zainoodin AM, Masdar MS. Active direct methanol fuel cell: An overview, *International Journal of Hydrogen Energy*. 2020;45:38. doi:10.1016/j.ijhydene.2020.04.202

6. Singh M, Sharma HM, Gupta RK *et al.* Recent advancements and prospects in noble and non-noble electrocatalysts for materials methanol oxidation reactions. *Discover Nano. 2024;***19**:128. doi:10.1186/s11671-024-04066-w
7. Zhao X, Yin M, Ma L, *et al*. Recent advances in catalysts for direct methanol fuel cells. *Energy Environ Sci.* 2011;4:2736. doi:10.1039/C1EE01241J
8. Zheng W, Suominen A, Tuominen A. Discussion on the challenges of DMFC catalyst loading process for mass production. *Energy Procedia.* 2012;28:78. doi:10.1016/j.egypro.2012.08.037
9. Cao L, Scheiba F, Roth C, *et al*. Novel Nanocomposite Pt/RuO_2· xH_2O/Carbon Nanotube Catalysts for Direct Methanol Fuel Cells. *Angew Chem Int Ed.* 2006;45:5315. doi:10.1002/anie.200600877
10. Song H, Qiu X, Guo D, Li F. Role of structural H_2O in TiO_2 nanotubes in enhancing Pt/C direct ethanol fuel cell anode electrocatalysts. *J Power Sources.* 2008;178:97. doi:10.1016/j.jpowsour.2007.11.063
11. Qasim MY, Munawar T, Alam MM, *et al*. Facile synthesis of MOF-derived carbon-supported LaZn@C nanocomposite as an efficient electrode material for supercapacitor, *J Alloys and Compd.*2024;1007:176402. Doi:10.1016/j.jallcom.2024.176402
12. Park CH, Louie SG. Tunable excitons in biased bilayer graphene. *Nano Lett.* 2010;10:426. doi:10.1021/nl903397a
13. Alias NN, Shazni MA, Haniff M, *et al.* A Review of Graphene-Based Electrocatalysts for Methanol and Hydrogen Oxidation: Design Strategies, Performance, and Prospects. *Energy & Fuels.* 2026;*40*:9. doi:10.1021/acs.energyfuels.5c05693
14. Schedin F, Geim AK, Morozov SV, *et al*. Detection of individual gas molecules adsorbed on graphene. *Nat Mater.* 2007;6:652. doi:10.1038/nmat1967
15. Huang H, Wang X. Recent progress on carbon-based support materials for electrocatalysts of direct methanol fuel cells. *J Mater Chem A.* 2014;2:6266. doi:10.1039/C3TA14674D
16. Zhou X, Qiao J, Yang L, Zhang J. A review of graphene-based nanostructural materials for both catalyst supports and metal-free catalysts in PEM fuel cell oxygen reduction reactions. *Adv Energy Mater.* 2014;4:130152. doi:10.1002/aenm.20130152
17. Mahmood N, Zhang C, Yin H, Hou Y. Graphene-based nanocomposites for energy storage and conversion in lithium batteries, supercapacitors and fuel cells. *J Mater Chem A.* 2014;2:15. doi:10.1039/C3TA13374A
18. Guo S, Dong S. Graphene nanosheet:

synthesis, molecular engineering, thin film, hybrids, and energy and analytical applications. *Chem Soc Rev.* 2011;40:2644. doi:10.1039/C0CS00174J

19. Kumar M, Kumar V, Mustafa S *et al*. Graphene-loaded nickel oxide nanocomposite as anode material for microbial fuel cell. *Biomass Convers Biorefin.* 2023:13:13245 doi:10.1007/s13399-022-02474-5
20. Liu M, Zhang R, Chen W. Graphene-supported nanoelectrocatalysts for fuel cells: synthesis, properties, and applications. *Chem Rev.* 2014;114:5117. doi:10.1021/cr400648j
21. Zhang J, Liu J, Peng Q, Wang X, Li Y. Nearly monodisperse Cu_2O and CuO nanospheres: preparation and applications for sensitive gas sensors. *Chem Mater.* 2006;18:867. doi:10.1021/cm052055b
22. Poonguzhali RV, Kumar ER, Arunadevi N *et al*. Natural citric acid assisted synthesis of CuO nanoparticles: Evaluation of structural, optical, morphological properties and colloidal stability for gas sensor applications. *Ceram Int*. 2022;48:18. doi: 10.1016/j.ceramint.2022.05.311.
23. Chang Y, Teo JJ, Zeng HC. Formation of colloidal CuO nanocrystallites and their spherical aggregation and reductive transformation to hollow Cu_2O nanospheres. *Langmuir.* 2005;21:1074. doi:10.1021/la047726h
24. Ali MJM, Radhy MM, Mashkoor SJ, *et al*. Synthesis and characterization of copper oxide nanoparticles and their application for solar cell, *Mater Today: Proc*. 2022;60:2. doi:10.1016/j.matpr.2021.10.250.
25. Singh J, Lee S, Tomar A, *et al*. Surfactant-Mediated Synthesis of Novel Mesoporous Hollow CuO Nanotubes as an Anode Material for Lithium-Ion Battery Application. *ChemistrySelect*. 2023;8. doi:10.1002/slct.202203755
26. Lu C, Qi L, Yang J, Zhang D, Wu N, Ma J. Simple template-free solution route for the controlled synthesis of $Cu(OH)_2$ and CuO nanostructures. *J Phys Chem B.* 2004;108:17825. doi:10.1021/jp046654+
27. Oviedo LR, Durzian DM, Montagner GE, *et al*.Supported heterogeneous catalyst of the copper oxide nanoparticles and nanozeolite for binary dyes mixture degradation: Machine learning and experimental design. *J Mol Liq*. 2024;402:124763. doi: 10.1016/j.molliq.2024.124763.
28. Li CC, Chang MH. Colloidal stability of CuO nanoparticles in alkanes via oleate modifications. *Mater Lett.* 2004;58:3903. doi:10.1016/j.matlet.2004.06.023
29. Hsieh CT, Chen JM, Lin HH, Shih HC. Field emission from various CuO nanostructures. *Appl Phys Lett.* 2003;83:3383. doi:10.1063/1.1625773
30. Poizot P, Laruelle S, Grugeon S, Dupont L, Tarascon JM. Nano-sized transition-metal oxides as negative-electrode materials for lithium-ion batteries. *Nature.* 2000;407:496. doi:10.1038/35035045
31. Mai YJ, Wang XL, Xiang JY, *et al*. CuO/graphene composite as anode materials for lithium-ion batteries. *Electrochim Acta.* 2011;56:2306. doi:10.1016/j.electacta.2010.11.013
32. Cao J, Chen Z, Xu J, Wang W, Chen Z. Mesoporous carbon synthesized from dual colloidal silica/block copolymer template approach as the support of platinum nanoparticles for direct methanol fuel cells. *Electrochim Acta.* 2013;88:184. doi:10.1016/j.electacta.2012.10.036
33. Rabbani AW, Naz G, Berd imurodov E, *et al*. Visible-Light-driven Photocatalytic Properties of Copper(I) Oxide (Cu2O) and Its Graphene-based Nanocomposites *Baghdad Sci J.* 2023;20:3. doi: 10.21123/bsj.2023.8476.
34. Kakati N, Maiti J, Lee SH, Yoon YS. Core shell like behavior of PdMo nanoparticles on multiwall carbon nanotubes and their methanol oxidation activity in alkaline medium. *Int J Hydrogen Energy.* 2012;37:19055. doi:10.1016/j.ijhydene.2012.10.020
35. Hummers WS Jr, Offeman RE. Functionalized graphene and graphene oxide: Materials synthesis. *J Am Chem Soc*. 1958;80:1339. doi:10.1021/ja01539a017
36. Sarkar C, Dolui SK. Synthesis of copper oxide/reduced graphene oxide nanocomposite and its enhanced catalytic activity towards reduction of 4-nitrophenol. *RSC Adv.* 2015;5:60763. doi:10.1039/C5RA08941A
37. Das D, Nath BC, Phukon P, Dolui SK. Synthesis and evaluation of antioxidant and antibacterial behavior of CuO nanoparticles.

Colloids Surf B. 2013;101:430. doi:10.1016/j.colsurfb.2012.07.002

38. Zhu J, Zeng G, Nie F, *et al*. Decorating graphene oxide with CuO nanoparticles in a water–isopropanol system. *Nanoscale.* 2010;2:988. doi:10.1039/B9NR00388K
39. Periasamy AP, Liu J, Lin HM, Chang HT. Synthesis of copper nanowire decorated reduced graphene oxide for electro-oxidation of methanol. *J Mater Chem* A. 2013;1:5973. doi:10.1039/C3TA01578E
40. Tran PD, Batabyal SK, Pramana SS, *et al*. A cuprous oxide–reduced graphene oxide (Cu_2O–rGO) composite photocatalyst for hydrogen generation: employing rGO as an electron acceptor to enhance the photocatalytic activity and stability of Cu_2O. *Nanoscale.* 2012;4:3875. doi:10.1039/C2NR30628A
41. Zhou C, Liu Z, Du X, *et al*. Hollow nitrogen-containing core/shell fibrous carbon nanomaterials as support to platinum nanocatalysts and their TEM tomography study. *Nanoscale Res Lett.* 2012;7:165. doi:10.1186/1556-276X-7-165